Validation and calibration of a spectroscopic technique for determination of gas plume temperature

Gerard P. Jellison*, David P. Miller
Northrop Grumman Information Technology - TASC,
11781 Lee Jackson Memorial Hwy., Suite 400, Fairfax, VA 22033

ABSTRACT

Results are reported from a continuing program of research into the physics and spectroscopy of heated stack plumes. Simultaneous thermocouple and spectrometer measurements are used to study sideways-directed plumes from an internal combustion engine and a propane-burning plume generator. A previously-reported result, that the ratio of optically thin signals from two CO_2 transitions can be used to determine plume temperature, is confirmed by comparison of thermocouple and spectrometer measurements over a wide range of temperatures. The basic physics of molecular emission and absorption of radiation is discussed and is used to calibrate the relationship between the spectroscopic ratio and plume temperature. The result is a spectroscopic plume temperature diagnostic that contains no adjustable parameters, and can be calibrated by use of published absorption spectra. Data relating to the accuracy of the technique are discussed.

Keywords: Gas plumes; effluent detection; infrared spectrometry; emissive; remote sensing

1. INTRODUCTION

Spectroscopic observations of stack plumes can, in principle, provide useful information about the identities, concentrations, and mass flow rates of the effluent gases. However, because infrared emission from molecules is a function of both temperature and concentration, the intensities of spectral features cannot be related to plume parameters in any simple way. If a reliable spectroscopic technique for temperature determination could be developed, however, these functional dependences could be unraveled. Remote determination of temperatures and molecular concentrations in plumes would then become much simpler.

The plume temperature estimation problem has been discussed in a number of published papers. Several of these publications report that, with the aid of certain assumptions regarding pixel uniformity and background clutter, temperature-emissivity separation algorithms can be used successfully with data cubes from imaging spectrometers.[1,2] Unfortunately, these algorithms require multiple pixels and so are not useful in conjunction with data from hand-held spectroradiometers. The alpha emissivity method has been applied to plumes,[3] but provides only relative emissivity with respect to a reference channel.[4] Existing techniques for single-spectrum determination of plume temperature generally require fine spectral resolution,[5,6,7,8,9] prior knowledge of plume emissivity and geometric factors,[10,11] or optically thick wavelengths.[12,13] There is still a need for a reliable temperature diagnostic under realistic field conditions.

In previously-reported work, the authors developed a new temperature diagnostic for plumes.[14] It was noted that the ratio between spectral intensities at widely-separated, optically thin wavelengths should depend on gas temperature in accord with well-established equations from molecular spectroscopy. Since the ratio between two optically thin measurements is independent of gas concentration, density fluctuations in the plume are normalized out by this technique. A further advantage is that fine spectral resolution is not required. This technique, already well-established in plasma diagnostics,[15] is a good candidate for field measurements on stack plumes. Preliminary experimental data indicated that this approach to plume temperature determination is both feasible and useful.

This paper provides further validation of this new temperature diagnostic over a wide range of gas temperatures. It also explains how the temperature diagnostic can be calibrated with the use of published library spectra. A companion paper discusses how absorption by plume gases and the intervening atmosphere affects the shapes of observed molecular spectra, and how these spectral contours can provide information on the thermal structure of plumes.[16]

* jellisog@sitac.org; phone 1 703 877-5013; fax 1 703 591-2437

Algorithms and Technologies for Multispectral, Hyperspectral, and Ultraspectral Imagery X, edited by Sylvia S. Shen, Paul E. Lewis, Proceedings of SPIE Vol. 5425 (SPIE, Bellingham, WA, 2004) · 0277-786X/04/$15 · doi: 10.1117/12.542289

2. THEORY OF PLUME SPECTROSCOPY

The widths and shapes of *individual* molecular emission bands are relatively temperature-independent over the temperature ranges found in stack plumes.[17] However, the ratio between emissions from two *different* transitions shows a temperature dependence that can easily be observed with field spectrometers. This section describes the physics that underlies the development and calibration of this temperature diagnostic. CO_2 transitions are emphasized, since the data presented in this paper involve this molecule.

2.1. Wavelengths and Energies of Molecular Transitions

Molecules exist in quantum states that correspond to various amounts of oscillatory or rotational energy. A molecule such as CO_2 can vibrate by bending or stretching. The molecule can also rotate about its center of mass. Each of these modes of motion is associated with an amount of energy that can be calculated by the well-established techniques of quantum mechanics.

As a linear triatomic molecule, CO_2 has two stretching modes: symmetric, in which the central carbon atom does not move, but the two oxygen atoms oscillate in and out; and asymmetric, in which all three atoms move. In addition, CO_2 has one bending mode. Figure 1 displays the vibrational energies of the CO_2 transitions of greatest interest in this study.[18] As seen in the figure, vibrational energies are typically on the order of hundreds or thousands of cm^{-1}. The wavelength of the radiation emitted in transitions between pure vibrational states is related to the vibrational energy ΔE_{vib} by

$$\lambda = \frac{ch}{\Delta E_{vib}} \tag{1}$$

where c is the speed of light and h is Planck's constant. As shown in Figure 1, wavelengths of vibrational transitions typically fall in the infrared part of the spectrum (tens of microns or less).

In addition to these vibrational modes, the spectrum of the CO_2 molecule is influenced by rotational energy, given in terms of the angular momentum quantum number J as

$$E_{rot} = BhcJ(J+1) \tag{2}$$

where B is a rotational constant inversely proportional to the molecule's moment of inertia. Differences between adjacent molecular rotational energy levels are considerably less than vibrational energies. However, for high J values, such as those relevant to this research, the total rotational energy can be comparable to the vibrational energy of the transition.

Molecules can vibrate and rotate at the same time. Spectral emissions from molecules in the near infrared generally involve changes in both the vibrational and the rotational quantum states. As a result, each of the vibrational levels shown in Figure 1 actually consists of a large number of finely-spaced rotational sublevels. The situation is illustrated in Figure 2, which shows a magnified view of two of the vibrational levels, along with some of the associated rotational sublevels. Each sublevel corresponds to a different J value. The rotation-vibration spectral lines correspond to transitions in which the vibrational quantum number v changes by ± 1, and J changes by -1, 0, or $+1$. Transitions in which the ΔJ between the lower and upper states is equal to -1, 0, and $+1$ are referred to as the P, Q, and R branches of the spectrum, respectively.

As an example, Figure 3 displays a high-resolution library spectrum of CO_2 in the vicinity of the 4.26 μm vibrational transition.[19] The figure shows the R and P branches; due to constraints on allowed quantum transitions, this transition has no Q branch.[20] As shown, the R and P branches flank the wavelength (4.26 μm) corresponding to the vibrational energy, and appear as a series of closely-spaced lines. Each of these lines corresponds to a different rotational ground state (J value). Due to the nuclear spin statistics of the CO_2 molecule, only even-numbered J states appear in the spectrum.[21]

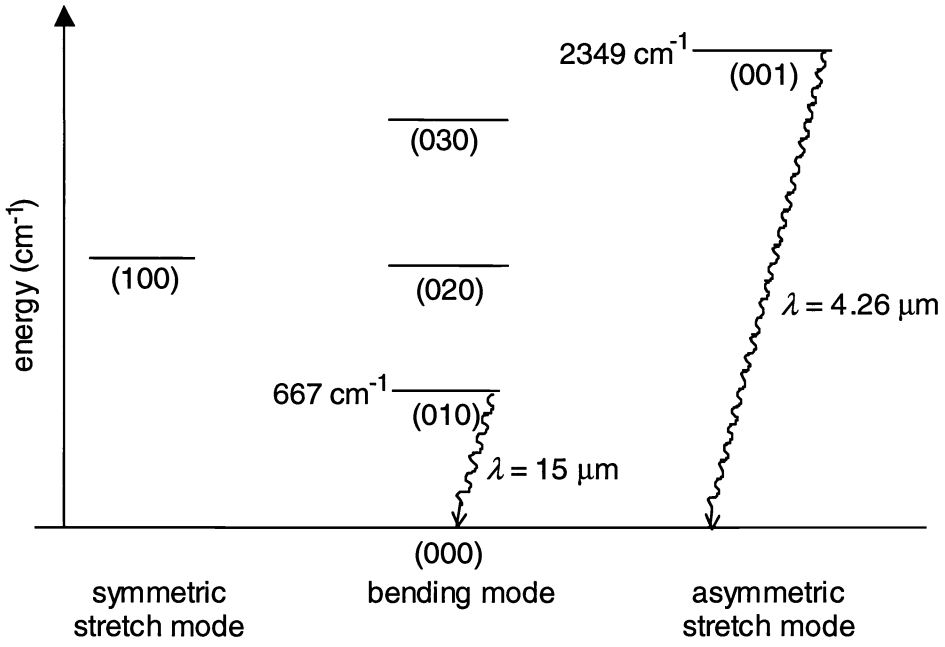

Figure 1. Vibrational energy levels of CO_2. Energies and wavelengths correspond to transitions near line centers (i.e., transitions between states with small values of angular momentum). Sublevels due to rotational effects are not shown.

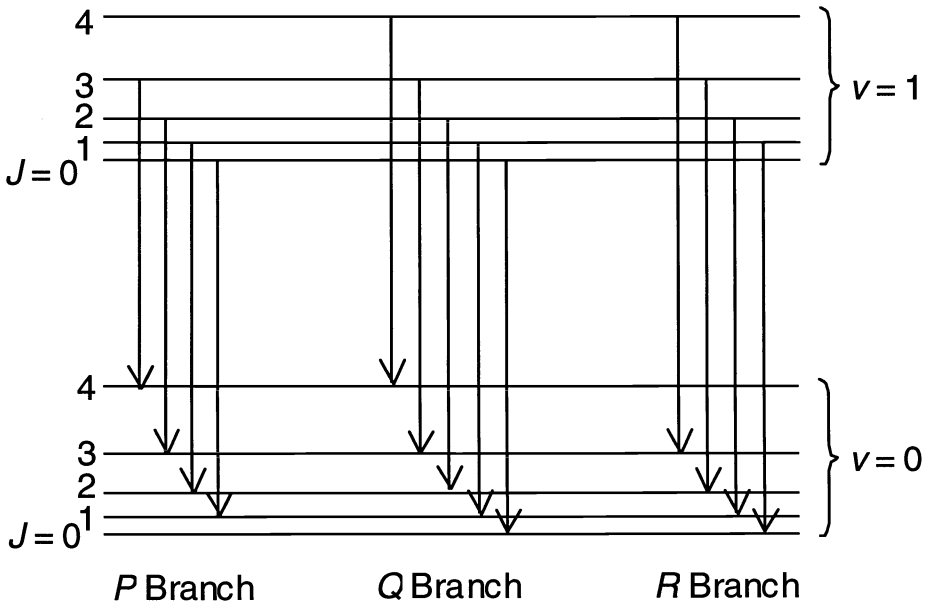

Figure 2. Rotation-vibration energy transitions. Energy levels are not to scale.

The spectroradiometer used for these measurements has insufficient spectral resolution to observe the fine lines caused by individual rotational transitions. The fine structure of the *R* and *P* branches is smeared out, allowing only the contours of the branches to be observed. This resolution limitation is not an impediment to the spectroscopic temperature diagnostic discussed in this paper.

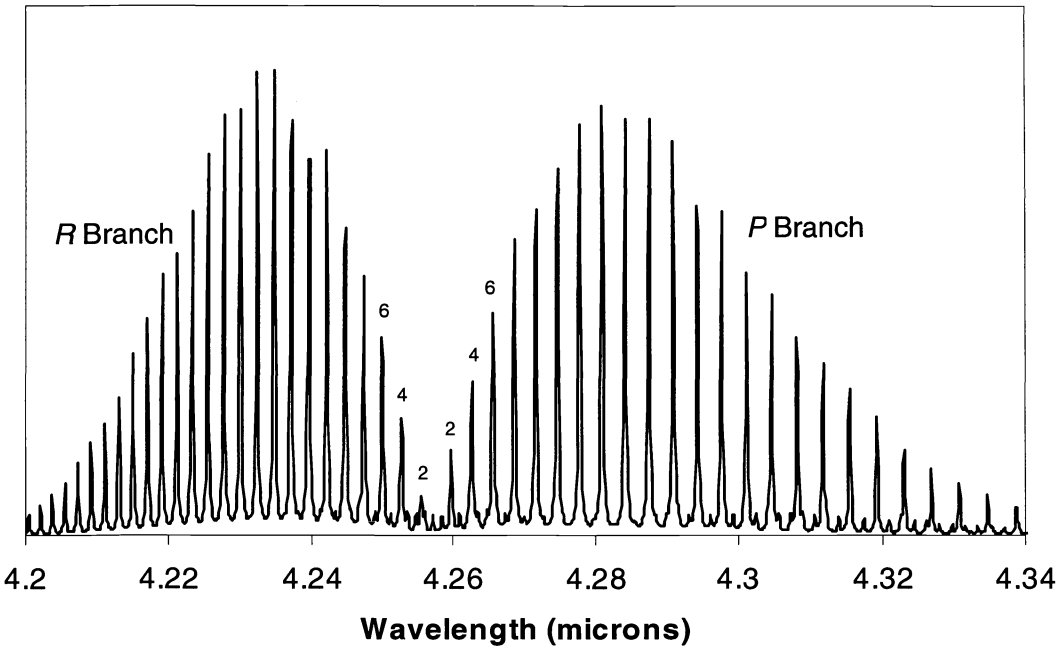

Figure 3. Details of CO_2 (001) → (000) spectrum. The lower J values of a few of the transitions are shown.

For a rotational-vibrational transition, the total energy difference ΔE_{total} has a vibrational and a rotational part:

$$\Delta E_{total} = \Delta E_{vib} + \Delta E_{rot} \approx \frac{hc}{\lambda_0} + BhcJ(J+1) \tag{3}$$

where λ_0 is the wavelength corresponding to the vibrational energy difference (approximately equal to the wavelength of a low-J transition). If the lower state of the transition is not the ground state, its rotational and/or vibrational energy must be included in ΔE_{total}. To a good approximation, the wavenumber of a transition is given by[22]

$$\upsilon = \upsilon_0 + (B' + B'')m + (B' - B'')m^2 \tag{4}$$

where υ_0 is the wavenumber of the line center (derived from the difference in vibrational energies of the upper and lower states), B' and B'' are the rotational constants for two states, and m = -J for the P branch and (J + 1) for the R branch.

The rotational constant of a molecule is inversely proportional to its moment of inertia. Since vibrational and rotational motions change the spacings between atoms, the moment of inertia depends, to a certain extent, on the vibrational and rotational quantum numbers. Such high-order corrections are small, however,[23] and in the energy calculations of this paper $B' \approx B''$ is assumed. The rotational constant can be determined by measuring the wavenumbers of the lines in Figure 3 corresponding to various J values and obtaining a fit to Eq. (4). For the purposes of this paper the rotational constant of CO_2 can be taken to be

$$B \equiv B' \approx B'' \approx 0.38 \text{ cm}^{-1} \tag{5}$$

2.2. Intensities of Molecular Transitions

Knowledge of the energies of molecular transitions allows one to compute the populations of the various excited states. However, the intensity of spontaneous emission at a given wavelength also depends on the intrinsic strength of the transition, which is not amenable to calculation from first principles. Fortunately, these intrinsic line strengths can be calibrated by use of readily-available laboratory spectra. Since such spectra are invariably taken in absorption rather than emission, it is necessary to understand the relationship between absorption and emission spectra.

2.2.1. Emission

The intensity (J/s) of spontaneous emission is[24]

$$I_{em} = N_2 h \upsilon_{12} A \tag{6}$$

where υ_{12} is the frequency of the radiation emitted in a transition from state 1 to state 2, N_2 is the population of the upper state, and the probability of a molecule undergoing a spontaneous emission is given by the Einstein coefficient

$$A = \frac{16\pi^3 \upsilon_{12}^3 |\mu_{12}|^2}{3\varepsilon_0 h c^3} \tag{7}$$

where ε_0 is the permittivity of free space and μ_{12} is the transition dipole moment. The population of the upper state is given by the Boltzmann factor

$$N_2 = \frac{N_0 g}{Q} \exp\left(-\frac{E_{total}}{kT}\right) \tag{8}$$

where N_0 is the total number of molecules, Q is the partition function, g is the degeneracy (the number of quantum states with energy E_{total}), k is Boltzmann's constant, and T is the temperature. The degeneracy of a molecular J state is

$$g = J(J+1) \tag{9}$$

The dipole moment factor in Eq. (7) is directly proportional to J. Therefore, the emitted intensity is

$$I_{em} \propto \upsilon_{12}^4 g J \exp\left(-\frac{E_{total}}{kT}\right) \tag{10}$$

This expression gives the signal obtained in a (presumed constant) interval $d\upsilon$ about υ_{12}. However, the spectrometer data discussed in this paper are expressed on a wavelength scale. Eq. (10) can be converted to wavelength using $d\upsilon = -cd\lambda / \lambda^2$ with the result

$$I_{em} \propto \lambda^{-6} g J \exp\left(-\frac{E_{total}}{kT}\right) \tag{11}$$

The ratio of signals emitted at two wavelengths, associated with two different vibrational transitions, is (assuming optically thin conditions at the wavelengths λ_1 and λ_2)

$$Ratio_{em} = F\left(\frac{\lambda_2}{\lambda_1}\right)^6 \left(\frac{g_1}{g_2}\right)\left(\frac{J_1}{J_2}\right)\left(\frac{\exp(-E_{total1}/kT)}{\exp(-E_{total2}/kT)}\right) \tag{12}$$

The normalizing factor F appears because the emission depends on direction cosine matrix elements that cannot be computed without a detailed quantum-mechanical analysis of the dipole moment factor in Eq. (7). For practical purposes, therefore, Eq. (12) must be normalized empirically, as described in the following sections.

2.2.2. Absorption

The F factor in Eq. (12), which depends on the intrinsic intensities of the two transitions in question, can be determined most easily by empirical means: finding the intensities of the two transitions at a known temperature. However, one

cannot blindly compare emission and absorption spectra, because the absorbance and emissivity behave differently as functions of temperature. This section develops the equations for absorption that are analogous to the emission equations in Section 2.2.1.

For absorption, the equation analogous to Eq. (6) is

$$I_{abs} = N_1 h \upsilon_{12} B \rho(\upsilon_{12}) \tag{13}$$

where $\rho(\upsilon_{12})$ is the radiation density at the frequency of interest and the Einstein absorption coefficient (different from the rotational constant B used earlier) is[25]

$$B = \frac{2\pi^2 |\mu_{12}|^2}{3\varepsilon_0 hc^2} \tag{14}$$

For absorption, the initial population N_1 is the population of the *lower* state. Therefore, if the vibrational energy of the lower state is zero, one uses only the *rotational* energy in the Boltzmann expression. The absorption equation analogous to Eq. (10) is then

$$I_{abs} \propto \upsilon g J \exp\left(-\frac{E_{rot}}{kT}\right) \tag{15}$$

If the vibrational energy of the lower state is not zero ("hot band"), the total energy of the lower state should be used in Eq. (15). The essential differences between the emission and absorption cases are the energy term in the Boltzmann expression and the different dependence on υ.

The library absorption spectra used in this study[19] are expressed on a wavenumber scale. Therefore, Eq. (15) already has the appropriate functional form, and conversion to wavelength can be done by the simple substitution $\upsilon = c/\lambda$. The ratio factor in absorption spectra is therefore

$$Ratio_{abs} \propto F\left(\frac{\lambda_2}{\lambda_1}\right)\left(\frac{g_1}{g_2}\right)\left(\frac{J_1}{J_2}\right)\left(\frac{\exp(-E_{rot1}/kT)}{\exp(-E_{rot2}/kT)}\right) \tag{16}$$

where the normalizing constant F is the same as in the emission case (Eq. (12)). This analysis therefore allows the spectroscopic ratio diagnostic for plume temperature to be calibrated using line strengths derived from absorbance spectra.

2.3. Application of Theory to Specific Transitions

The spectroscopic work reported in this report makes use of high-J transitions associated with the wavelengths 4.19668 μm and 14.5023 μm, chosen because they are well away from the line centers, and thereby avoid optical thickness problems. Examination of a detailed absorption spectrum (such as shown in Figure 2) allows the J values corresponding to these wavelengths to be deduced. Using the equations discussed in Section 2.1, one can then compute the energies of the upper states for these CO_2 wavelengths, using Eq. (3). The relevant parameters and energies are shown in Table 1.

Transition	J	g	E_{vib} (cm^{-1})	E_{rot} (cm^{-1})	E_{total} (cm^{-1})
4.19668 μm	56	3192	2349	1242	3591
14.5023 μm	26	702	667	266	933

Table 1. Spectroscopic parameters for CO_2 wavelengths used for temperature determination.

Using the parameter values in Table 1, the signal ratios for emission and absorption can be computed. From Eq. (12),

$$Ratio_{em} = F\left(\frac{\lambda_2}{\lambda_1}\right)^6\left(\frac{g_1}{g_2}\right)\left(\frac{J_1}{J_2}\right)\exp\left(\frac{E_{total2} - E_{total1}}{kT}\right) \tag{17}$$

and from Eq. (16),

$$Ratio_{abs} = F\left(\frac{\lambda_2}{\lambda_1}\right)\left(\frac{g_1}{g_2}\right)\left(\frac{J_1}{J_2}\right)\exp\left(\frac{E_{rot2} - E_{rot1}}{kT}\right) \tag{18}$$

The value of F is independent of wavelength (J value). For simplicity, we can absorb the factors that are the same in these two equations into a new constant F', yielding the equations

$$Ratio_{em} = F'\left(\frac{\lambda_2}{\lambda_1}\right)^6\exp\left(\frac{E_{total2} - E_{total1}}{kT}\right) \tag{19}$$

and

$$Ratio_{abs} = F'\left(\frac{\lambda_2}{\lambda_1}\right)\exp\left(\frac{E_{rot2} - E_{rot1}}{kT}\right) \tag{20}$$

Of course, the experimentally-determined value of F' will only apply only to the specific wavelengths given in Table 1.

(19) and (20) are the essential equations needed to perform temperature measurements using the spectroscopic ratio technique. The factor F' is evaluated from absorbance spectra in Section 4.1.

3. EXPERIMENTAL ARRANGEMENTS

3.1. Plume Sources

The spectral data discussed in this paper were collected using two controllable plume sources: the exhaust plume from a Ford Excursion™ engine and a plume from a portable propane-burning plume generator.

Details of the measurements on the Ford Excursion™ plume were given in Ref. 14. To provide a horizontal stack, 10-cm-diameter aluminum dryer vent hose was attached to the Ford tail pipe. A small aperture 1 meter from the stack exit allowed injection of volatile analytes, using a paint sprayer. This procedure allowed analyte spectra to be measured, and also cooled the plume, providing a range of plume temperatures without changing the spectrometer location. Flow velocity at the stack exit was 430 cm/s. Both upward- and downward-looking spectrometer data were obtained. For the downward-looking data, the plume was viewed against a blacktop background. The spectrometer measurements were supplemented by temperature data from several thermocouples that were placed at various positions in the flow.

Spectra from a portable plume generator were collected on a runway at the Mid-Way Regional Airport near Waxahachie, Texas from April 6 to April 11, 2003. The plume generator was constructed and operated by AeroSurvey, Inc. Its base unit contains a centrifugal blower that feeds a combustion plenum, in which resides a liquid propane burner. Heated gas from the combustion plenum is fed into an elbow that redirects the gas into a 19-in. diameter stack. Plume temperature is regulated by adjusting the propane delivery pressure to the burner. For the measurements discussed in this paper, the stack was operated in a horizontal configuration, with the plume being ejected along the wind direction. This configuration provided a sideways-directed plume, sometimes referred to as a "momentum jet" since the plume dynamics are initially dominated by the momentum with which the gas is ejected from the stack. The horizontal configuration provided easy access to the plume. In particular, it allowed the spectrometer to be placed near the plume, minimizing absorption effects from intervening atmosphere. Figure 4 shows the portable plume generator in its horizontal configuration.

Figure 4. Waxahachie portable plume generator with horizontal stack configuration. Thermocouple array is on the right side of the figure.

3.2. Instrumentation

The spectral measurements were made using a Designs and Prototypes (D&P), Inc. MicroFTIR Model 101 spectroradiometer. Useful spectral data were obtained in the range from 3 to 18 μm. The spectral resolution at 10 μm was approximately 40 nm. The single scan time was 16 seconds.

Thermocouple readings were taken from the vehicle exhaust plumes and the Waxahachie plumes. For the vehicle exhaust measurements, eight thermocouples were positioned at various locations in the plume; distances from the outlet ranged from 0 to 93 cm. Temperatures were recorded manually. During the Waxahachie collection a large three-dimensional thermocouple array was used, as seen in Figure 4. The thermocouples were positioned on a wire grid that was supported by a 2 m x 2 m PVC framework. Two planes of thermocouples were used, giving readings at two downstream positions. Electrical outputs from the thermocouples were transmitted to daisy-chained solid-state modules, and then to a computer for automatic recording. A fresh set of readings from all the thermocouples was recorded every two seconds.

For the Waxahachie measurements, the spectrometer was positioned inside the thermocouple array, giving readings at a location roughly midway between the two thermocouple planes.

4. MEASUREMENT RESULTS AND ANALYSIS

4.1. Calibration of Spectroscopic Temperature Equation Using Absorbance Data

The calibration factor F' used in Eqs. (19) and (20) was determined using PNNL library CO_2 absorbance data.[19] Absorbance values were available at three temperatures: 278 K, 298 K, and 323 K. Figure 5 shows the measured ratio of absorbances at the wavelengths 4.19668 μm and 14.5023 μm, along with a best-fit curve computed from Eq. (20) with $F' = 19.6$. This value is used in the following analysis of Waxahachie and vehicle plume data.

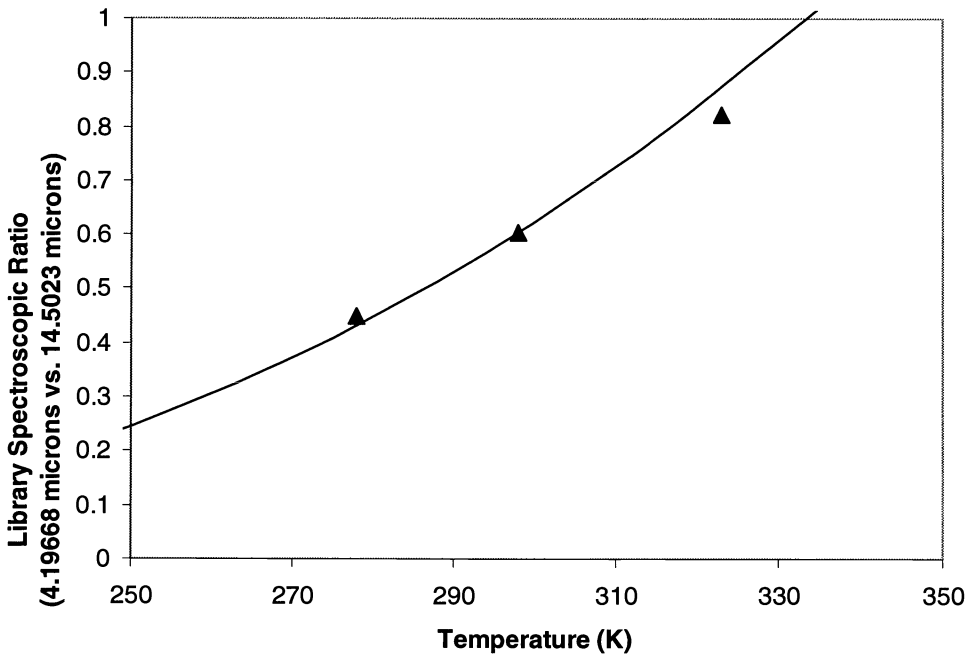

Figure 5. Ratio of library absorbance spectrum values in vicinity of 4.19668 and 14.5023 microns (points) with theoretical prediction (curve).

4.2. Experimental Verification of Temperature Diagnostic (Waxahachie and Vehicle Plume Data)

With the calibration factor F' determined as described in the preceding section, the plume temperature can be computed from spectrometer data. The procedure is to find the emission at two wavelengths corresponding to known molecular transitions, and to determine the temperature with the use of Eq. (19).

This procedure requires some forethought and care. With a dense plume, the two wavelengths chosen may need to be far from the line center to achieve optically thin emission. If there was a significant path length between the spectrometer and the plume, the wavelengths should be far enough onto the spectral wings that atmospheric absorption is not a problem. If possible, only one molecular transition should be active at each of the two wavelengths. After some trial and error, wavelengths of 4.19668 μm and 14.5023 μm were found to be appropriate for use with the collected data.

In order to obtain an accurate value for plume emission, the background signal must be removed from the spectrometer measurements. For the vehicle plume data, the background was asphalt; for the Waxahachie data, the background was sky. In most cases, the subtraction of the background signal was uncomplicated.

However, difficulties were encountered with the highest-temperature (606 K) Waxahachie data point. The 606 K spectrum showed the usual CO_2 emission line in the vicinity of 15 μm, but it was superimposed on a continuum spectrum that did not appear with lower-temperature plumes. A strong emission from water bands is not surprising at high temperature, since the plume generator used water for cooling. With the assumption that this continuum is derived from water bands, the CO_2 emission was estimated using an assumed "floor" at the approximate location of the underlying continuum emission, giving results at 606 K that appear consistent with the rest of the data. However, because of this correction factor, the highest-temperature point should be considered less reliable than the others.

With appropriate wavelengths chosen, spectroscopically-determined temperatures can be compared with thermocouple "ground truth." Figure 6 shows spectroscopic intensity ratios plotted against corresponding thermocouple temperatures. Crosses represent data from the vehicle exhaust plume experiments. Squares represent Waxahachie data for which temperatures were determined from the thermocouple array. Triangles represent data for which temperature was found from a hand-held thermocouple positioned in the hottest part of the plume. The curve is the theoretical prediction from Eq. (19), using $F' = 19.6$ as determined in Section 4.1. Agreement between theory and experiment is very good, indicating that plume temperature can indeed be determined by inserting the observed intensity ratio into Eq. (19).

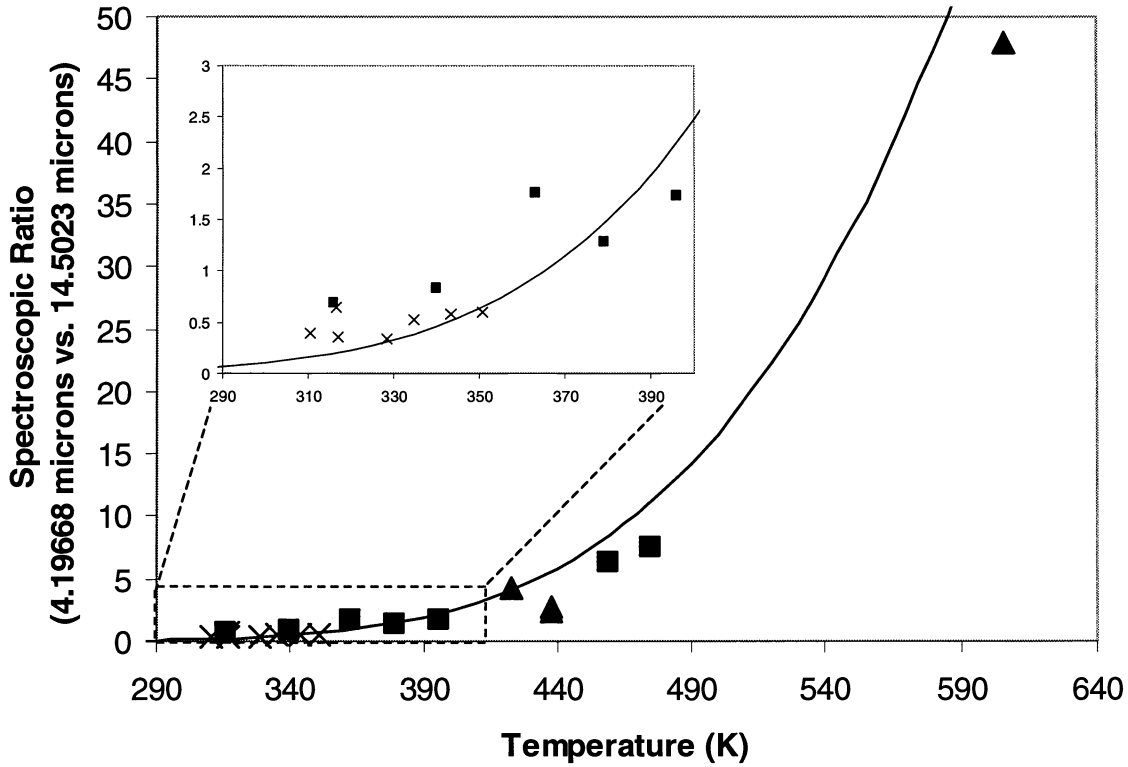

Figure 6. Ratio of signal at two wavelengths vs. thermocouple temperature measurements.

The inset region of Figure 6 shows a closeup view of the low-temperature portion of the curve. The vehicle plume data and low-temperature Waxahachie data are in good agreement with each other as well as with the theoretical curve.

The comparison between thermocouple and spectroscopic temperatures is quantified in Table 2. The "error" values in the table are the differences between the two temperatures. It should be remembered, of course, that the thermocouple measurements undoubtedly have some associated error; hence, the discrepancies are not solely due to uncertainties in the spectroscopic temperatures. The root-mean-square error is 24 K.

TC Temperature	Spectroscopic Temperature	Error
316	353.1	-37.1
340	359.0	-19.0
363	386.2	-23.2
379	374.4	4.6
396	385.8	10.2
423	423.5	-0.5
438	397.2	40.8
438	403.3	34.7
459	443.9	15.1
475	453.0	22.0
606	581.3	24.7

Table 2. Thermocouple and spectroscopic temperature comparison (Waxahachie data).

For the points around 400 K, the agreement between the thermocouple and spectroscopic temperatures is excellent. It appears that some systematic error may be present; for low-temperature points the spectroscopic temperatures are higher than the thermocouple values, and vice versa for high-temperature points. Examination of Figure 6 shows that the vehicle plume data points (crosses) follow the same pattern; they are low-temperature points, and almost all of them lie above the theoretical curve. Identifying the source of this systematic error in subsequent research may improve the accuracy of the spectroscopic temperature diagnostic.

5. CONCLUSIONS

The goal of this research, validation of the spectroscopic ratio technique for temperature determination, was achieved by accumulating plume spectra over a wide range of temperatures. In the previously-reported work (Ref. 14), thermocouple data were available only up to 360 K; the data presented herein extended this range up to 606 K. The spectroscopic ratio vs. temperature dependence followed the predictions of the Maxwell-Boltzmann theory over this entire range.

Apart from the variation with temperature, the actual value of the spectroscopic ratio depends on the intrinsic strengths of the emissions at the two wavelengths. In Ref. 14, the curve of spectroscopic ratio vs. temperature had to be empirically scaled to match the data, implying that temperature measurement required a large number of measurements to trace out the curve (in the absence of ground truth). This paper develops a calibration procedure using library spectra, demonstrating that a laborious scaling process is not necessary. The conclusion is that even a single remotely-sensed spectrum can provide a determination of plume temperature, provided only that two molecular transitions can be observed and compared with library spectra.

The current results support the conclusion that measurement of spectroscopic ratios, in conjunction with physics-based analysis, can provide estimates of plume temperatures. Using the calibration equations presented in this report, the temperature can be found from a single measurement by solving Eq. (19) to obtain

$$T = \frac{E_{total2} - E_{total1}}{k \ln\left[\dfrac{Ratio}{F'(\lambda_2/\lambda_1)^6}\right]} \tag{21}$$

As this equation shows, a significant advantage of the spectroscopic ratio technique is the logarithmic dependence of the derived temperature on the measured quantity (the ratio of emission at the two wavelengths). The effect of measurement errors is thereby minimized.

Another Waxahachie collection is scheduled for 2004. Planned experiments include work with high-temperature plumes to fill the data gap between 500 K and 600 K. A high priority is the injection of volatile substances to provide spectral transitions associated with plume gases other than CO_2. Some preliminary experiments have been made with methanol and ethanol, and analysis of the data suggests that the spectroscopic ratio technique can provide accurate temperatures using these gases. Additional data are needed, however to confirm this assertion. It is hoped that further experimentation and analysis along these lines will provide improved understanding of both the capabilities and limitations of hyperspectral measurements of plumes and gas releases.

ACKNOWLEDGEMENTS

The Waxahachie collection was a collaborative effort between the Defense Intelligence Agency (DIA) Office for MASINT Technology Integration and Fielding (DTT), Los Alamos National Laboratory (LANL), and the Environmental Protection Agency (EPA) Region-7, and was conducted under the auspices of the EPA. Herbert Mitchell originated many of the experimental procedures discussed in this paper, took the spectrometer measurements, and participated in all phases of the analysis. Without his contributions and generosity, this paper would not have been possible. Important assistance at Waxahachie was provided by experiment design leads Robert Kroutil (LANL) and Mark Thomas (EPA), as well as participants from AeroSurvey, Airborne Imaging, and McKinzie Environmental. Craig Miller and Joe Leckie provided able assistance with the experimental setup and measurements. The authors are grateful to the management of the former SITAC, in particular Lt. Col. Eric Stewart, for encouragement and support.

BIBLIOGRAPHY

1. Hayden, A. and Noll, R., "Remote Trace Gas Quantification Using Thermal IR Spectroscopy and Digital Filtering Based on Principal Components of Background Scene Clutter," *Algorithms for Multispectral and Hyperspectral Imagery III*, Proc. SPIE vol. **3071**, pp. 158-168 (1997).
2. Young, S. J., "Detection and Quantification of Gases in Industrial-Stack Plumes Using Thermal-Infrared Hyperspectral Imaging," The Aerospace Corporation, El Segundo, CA, ATR-2002 (8407)-1 (2002), pp. 53-55.
3. Thomas, M. J., Lewis, P. E., Kroutil, R. T., Combs, R. J., Small, G. W., Zywicki, R. W., Stageberg, D. L., Chaffin, C. T., and Marshall, T. L., "Infrared Detection and Analysis of Vapor Plumes Using an Airborne Sensor," *Algorithms and Technologies for Multispectral, Hyperspectral, and Ultraspectral Imagery VIII*, Proc. SPIE vol. **4725**, pp. 47–64 (2002).
4. Li, Z.-L., Becker, F., Stoll, M. P., and Wan, Z., "Evaluation of Six Methods for Extracting Relative Emissivity Spectra from Thermal Infrared Images," *Remote Sens. Environ.*, vol. **69**, pp. 197-214 (1999).
5. Chan, S. H., Lin, C. C., and Low, M. J. D., "Analysis of Principles of Remote Sensing and Characterization of Stack Gases by Infrared Spectroscopy," *Environ. Sci. Technol.*, vol. **7**, pp. 424-427 (1973).
6. Herget, W. F. and Brasher, J. D., "Remote Fourier Transform Infrared Air Pollution Studies," *Opt. Eng.*, vol. **19**, pp. 508-514 (1980).
7. Herget, W. F., "Remote and Cross-Stack Measurement of Stack Gas Concentrations Using a Mobile FT-IR System," *Appl. Opt.*, vol. **21**, pp. 635-641 (1982).
8. Gross, L. A., Griffiths, P. R., and Sun, J. N.-P., "Temperature Measurement by Infrared Spectroscopy," in *Infrared Methods for Gaseous Measurements*, J. Wormhoudt, editor, Marcel Dekker, Inc., New York, pp. 81-137 (1985).
9. Haus, R., Schäfer, K., Bautzer, W., Heland, J., Mosebach, H., Bittner, H., and Eisenmann, T., "Mobile Fourier-Transform Infrared Spectroscopy Monitoring of Air Pollution," *Appl. Opt.,* vol. **33**, pp. 5682-5689 (1994).
10. Prengle, H. W., Morgan, C. A., Fang, C.-S., Huang, L.-K., Camapani, P., and Wu, W. W., "Infrared Remote Sensing and Determination of Pollutants in Gas Plumes," *Environ. Sci. & Technol.*, vol. **7**, pp. 417-423 (1973).
11. Prengle, H. W., Mahagaokar, U., and Tse, S.-K., "Thermal and Momentum Structure of an Emerging Plume by Remote Sensing," in *Infrared Methods for Gaseous Measurements*, J. Wormhoudt, editor, Marcel Dekker, Inc., New York, pp. 47-79 (1985).
12. Solomon, P. R., Morrison, P. W., and Serio, M. A., "Fourier Transform Infrared Spectroscopy for Process Monitoring and Control," *Industrial, Municipal, and Medical Waste Incineration Diagnostics and Control*, Proc. SPIE vol. **1717**, pp. 104-115 (1992).
13. Hilton, M., Lettington, A. H., and Mills, I. A., "Quantitative Analysis of Remote Gas Temperatures and Concentrations from Their Infrared Emission Spectra," *Meas. Sci. Technol.*, vol. **6**, pp. 1236-1241 (1995).
14. Jellison, G. P., Mitchell, H. J., and Miller, D. P., "Theory, Modeling, and Measurements of Gas Plumes," *Algorithms and Technologies for Multispectral, Hyperspectral, and Ultraspectral Imagery IX*, Proc. SPIE vol. **5093**, pp. 172-183 (2003).
15. Griem, H. R., *Principles of Plasma Spectroscopy*, Cambridge University Press, Cambridge (1997), p. 281.
16. Jellison, G. P., Mitchell H. J., Miller, D. P., "Plume Structure and Dynamics from Thermocouple and Spectrometer Measurements," *Algorithms and Technologies for Multispectral, Hyperspectral, and Ultraspectral Imagery X*, Proc. SPIE vol. **5425** (2004).
17. Chan, S. H., Lin, C. C., and Low, M. J. D., "Analysis of Principles of Remote Sensing and Characterization of Stack Gases by Infrared Spectroscopy," *Environ. Sci. Technol.*, vol. 7, pp. 424-427 (1973).
18. Milonni, P. W. and Eberly, J. H., *Lasers*, Wiley, New York (1988), p. 438.
19. *Infrared Spectral Library, Version 7*, Pacific Northwest National Laboratory, Richland, WA (2002).
20. Levine, I. N., *Molecular Spectroscopy*, Wiley-Interscience, New York (1975), p. 259.
21. Duxbury, G., *Infrared Vibration-Rotation Spectroscopy: From Free Radicals to the Infrared Sky*, Wiley, New York (2000), p. 174.
22. Brown, J. M., *Molecular Spectroscopy*, Oxford University Press, Oxford (1998), p. 48.
23. Harmony, M. D., "Molecular Spectroscopy and Structure," in *Physics Vade Mecum*, H. L. Anderson, editor, American Institute of Physics, New York, pp. 223-225 (1981).
24. Brown, J. M. (1998), p. 16.
25. Brown, J. M. (1998), p. 16.